Hysteresis Model of Structural Materials under Repeated Elasto-Plastic Deformation

AUTHOR(S):

KOIKE, Takeshi; IZUNAMI, Ryuji; KAMEDA, Hiroyuki

CITATION:

KOIKE, Takeshi ...[et al]. Hysteresis Model of Structural Materials under Repeated Elasto-Plastic Deformation. Memoirs of the Faculty of Engineering, Kyoto University 1975, 36(4): 473-487

ISSUE DATE:

1975-03-25

URL:

http://hdl.handle.net/2433/280963

Hysteresis Model of Structural Materials under Repeated Elasto-Plastic Deformation

By

Takeshi KOIKE*, Ryuji IZUNAMI** and Hiroyuki KAMEDA*

(Received June 29, 1974)

Synopsis

This study has been attempted in order to simulate a plastic fatigue failure process and transition of hysteresis loops under a cyclic elasto-plastic deformation.

The hysteresis model proposed herein consists of continuously distributed parallel elements. It can display the fatigue failure process of material which hardens in its initial stage, and deteriorates in the second stage unitil complete failure occurs.

The numerical results based on the model are compared with the experimental results of a plastic bending fatigue test on SS 41 H-section steel beams.

1. Introduction

Many hysteresis models have been proposed in order to simulate and actual response of structures under large amplitude cyclic loadings; for example, bi-linear model, tri-linear model, Ramberg-Osgood model and so forth.

As large amplitude cyclic loading is repeated, plastic flow is accumulated in the structural material, and it is gradually softened. It must be noted that such structural behvaior under large amplitude cyclic loading should be reflected in setting up hysteresis loop models. By doing so, the hysteresis loop model under large amplitude cyclic loading can be physically meaningful.

There are a few macroscopic concepts in the fatigue failure mechanism, for example, that introduced by E. Orowan[1] in 1939. He proposed that fatigue occurs when the increasing local stress level due to strain hardening exceeds a certain level.

This idea is efficient enough to deal with the failure criterion on the macroscopic scale, though it may not always represent the true internal mechanism of the material.

Herein, the microscopic failure mechanism is not considered, but it is only

* Dept. of Transportation Engineering

** Dept. of Civil Engineering present adress: Kobe city office

assumed that randomly distributed latent defects existing in the material are elementary sources of fatigue failure. It has been attempted to simulate the plastic fatigue failure process and transition of hysteresis loops under a cyclic elasto-plastic deformation.

2. Model of Failure Mechanism

2.1. General remarks

Under strong cyclic loading, the hysteresis loops may harden or soften progressively. It is necessary from the view point of cumulative fatigue failure to take account of this effect, for example, in the elasto-plastic response analysis of structures subjected to a strong earthquake motion.

In the plastic fatigue failure process of engineering materials, strain-hardening takes place within the first few cycles of loading[2),3)]. Then, gradual deterioration follows until the fatigue failure occurs at a specific cycle, N. These characteristics are considered to arise from many complicated behaviors of various defects, such as dislocations, cracks, interstitial clusters or grain boundaries[4)].

Now, we suppose that material containing many kinds of defects can be approximately regarded as a class of continuously distributed elements with their own ultimate strength, depending on their size and kind of defects. Then, the local failure of each element will occur when the increasing stress applied to it, due to cumulative strain-hardening, exceeds its ultimate strength.

These considerations lead to the one dimensional model of materials, which consists of continuously distributed parallel fibre elements, each having a pair of yielding and ultimate strengths as described in 2.1. The abscissa in Fig. 1 represents strain e and the ordinate, stress s, in the element.

Each element is specified by the yield strength s_y, the ultimate strength s_u, and the stiffness k and μk in the elastic and plastic domains, respectively.

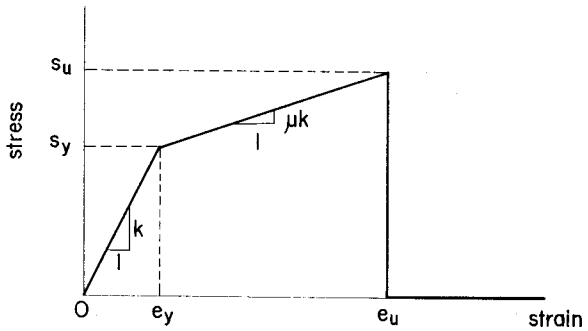

Fig. 1. Constitutive relation of a single element.

A local failure occurs when the applied stress s, reaches the ultimate stress level s_u, so that the failure criterion of the element is given by the following equation.

$$s = s_u \qquad \cdots\cdots(1)$$

It is noted that eq. (1) requires the ultimate strength be constant through the plastic fatigue failure process. This assumption is said to be aceeptable[5] for a large amplitude plastic fatigue failure, which is the case dealt with herein.

The sectional force of the material is given by the resultant stress of the surviving elements.

2.3. Parameters

The element is specified by the elastic modulus k, the hardening factor μ, the yield strength s_y and the ultimate strength s_u. Since the failure process would not be sensitive to the material constants k and μ, these two parameters are assumed to have the same values through all elements.

Other material constants, s_y and s_u, however, are considered to be affected by existing defects in the material. Then, we introduce a two dimensional distribution function $\phi(s_u, s_y)$ satifsying the following conditions;

$$\text{(i)} \quad \varphi(s_u, s_y) = \varphi(-s_u, -s_y) \qquad \cdots\cdots(2)$$

$$\text{(ii)} \quad s_u \geqslant s_y \qquad \cdots\cdots(3)$$

$$\text{(iii)} \quad \iint_\Omega \varphi(s_u, s_y) ds_u ds_y = 1 \qquad \cdots\cdots(4)$$

The equality in eq. (3) represents brittle materials.
The mean value of the yield strength of the material is given by

$$\bar{s}_y = \int_0^\infty \int_0^\infty s_y \varphi(s_u, s_y) ds_u ds_y \qquad \cdots\cdots(5)$$

The non-dimensional stress σ and the modified strain ε can be defined using eq. (5) as follows.

$$\sigma = s/\bar{s}_y \qquad \cdots\cdots(6)$$

$$\varepsilon = ke/\bar{s}_y \qquad \cdots\cdots(7)$$

in which e is the applied strain, and k is the elastic modulus. ε approximately represents the mean ductility factor of the material. In the same manner, the yield strain e_y and the ultimate strain e_u are redefined as follows:

$$\varepsilon_y = ke_y/\bar{s}_y \qquad \cdots\cdots(8)$$

$$\varepsilon_u = ke_u/\bar{s}_y \qquad \cdots\cdots(9)$$

The constitutive relations shown in Fig. 1 are classified in the case of monotonic loading as follows.

(i) $0 \leq \varepsilon \leq \varepsilon_y$; $\sigma = \varepsilon$ .....(10)

(ii) $\varepsilon_y \leq \varepsilon \leq \varepsilon_u$; $\sigma = \mu(\varepsilon - \varepsilon_y) + \sigma_y$ .....(11)

(iii) $\varepsilon > \varepsilon_u$; $\sigma = 0$ .....(12)

2.4. Hardening rate factor ζ

There are many conventional hysteresis models that can display stationary loops independent of loading history. But they are not adequate enough to represent the plastic fatigue failure process, which deteriorates depending upon the cycles until the fatigue failure takes place.

In this study, a physically meaningful hysteresis model, including a macroscopic fatigue mechanism, is presented.

It may be necessary to examine some possible paths in the n th cycle of the hysteresis loop as shown in Fig. 2.

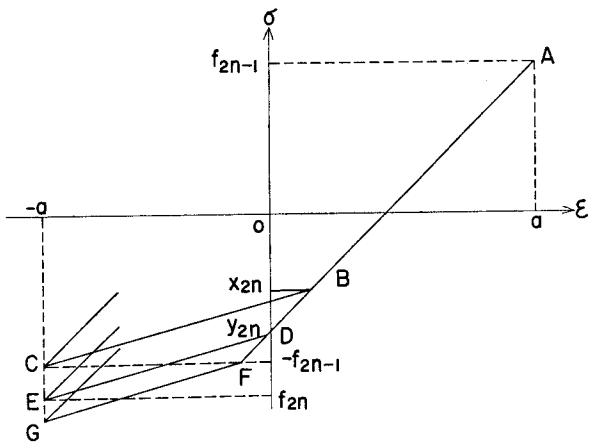

Fig. 2. Some possible paths of hysteresis loop.

The path ABC corresponds to the stable bi-linear hystereis loop, where stress levels at points A, B and C are f_{2n-1}, x_{2n}, and $-f_{2n-1}$, respectively.

The path AFG adopts $-f_{2n+1}$ as the yield stress level at point F, which is the same stress level as at point A. The path AFG makes the plastic fatigue failure process follow the monotonic tensile failure mechanism illustrated in Fig. 1.

The two paths discussed above are extreme cases of stable hysteresis and progressive strain hardening. In practical materials, the path would be somewhere between them.

Actually, a path ADE could be introduced. To represent this path, a non-dimensional parameter ζ_n is defined as

$$\zeta_n(\alpha) = (x_{2n}-y_{2n})/(x_{2n}-f_{2n-1}) \quad \cdots\cdots(13)$$

in which α is the input strain amplitude, y_{2n} is the stress level at D in Fig. 2. The parameter ζ_n will be called the strain hardening rate factor in this sudy.
This hardening rate factor, characterizing the development of plastic fatigue failure, represents the ascending rate of stress level per cycle of plastic strain in each element.

Parameter ζ_n generally takes a value in the range [0, 1]. The path BC in Fig. 2 corresponds to $\zeta_n=0$, and the path FG, to $\zeta_n=1$.

3. Monotonic loading curve

The monotonic loading curve of a material with a finite section can be formulated by using the element model introduced in the previous chapter.

The material is treated as a parallel assembly of such elements with s_y and s_u distributed in accordance with eqs. (2)–(4). Given the ductility factor ε, each element is in the elastic range, the plastic range, or in complete fracture, depending upon the magnitude of ε relative to σ_y and σ_u;

(i) $\sigma_y \geqslant \varepsilon \quad ; \sigma = \varepsilon \quad \cdots\cdots(14)$

(ii) $\sigma_y \leq \varepsilon,\ \mu(\varepsilon-\varepsilon_y)+\sigma_y \leqq \sigma_u;\ \sigma = \mu(\varepsilon-\varepsilon_y)+\sigma_y \quad \cdots\cdots(15)$

(iii) $\sigma_u \leq \mu(\varepsilon-\varepsilon_y)+\sigma_y \quad ; \sigma = 0 \quad \cdots\cdots(16)$

By integrating all elements over the material, the nondimensional sectional force $F(\varepsilon)$ is obtained as follows:

$$F(\varepsilon) = \int_0^\infty \int_{\mu(\varepsilon-\varepsilon_y)+\sigma_y}^\infty \{\mu(\varepsilon-\varepsilon_y)+\tau_y\}\varphi(\sigma_u, \sigma_y)d\sigma_u d\sigma_y + \int_\varepsilon^\infty \int_{\sigma_y}^\infty \varepsilon\varphi(\sigma_u, \sigma_y)d\sigma_u d\sigma_y \quad \cdots\cdots(17)$$

If the ductility factor ε increases infinity, $F(\varepsilon)$ eventually shirinks to zero, which means the complete failure of the material.

Eq.(17) simulates the nominal strain and stress relation in the tensile test of the material. Under the assumption that the shrinking rate of the cross section is proportional to the number of fractured elements, the real strain and stress relation is given as follows,

$$F^*(\varepsilon) = F(\varepsilon)/\{1-\int_0^\varepsilon \int_{\sigma_u}^\infty \{\mu(\varepsilon-\varepsilon_y)+\sigma_y\}\varphi(\sigma_u, \sigma_y)d\sigma_u d\sigma_y\} \quad \cdots\cdots(18)$$

4. Hysteresis loop

The hysteresis loop under a repeated constant strain amplitude is formulated.

4.1. Behavior of a single element

The first cycle of an element is shown in Fig. 3. The bold line in this figure represents an element in the plastic stage, with the yield level σ_y less than the applied strain amplitude a given in terms of the ductility factor.

The maximum stress f_1 and the yield stress y_1 (which are nondimensional) of this element are given by

$$f_1 = (1-\mu)\sigma_y + \mu a \qquad \cdots\cdots\cdots\cdots(19)$$

$$y_1 = \sigma_y \qquad \cdots\cdots\cdots\cdots(20)$$

Another element in the elastic stage with a higher yield level σ_y than the amplitude a behaves as shown by the thin line, where any hysteresis loop does not appear and the element repeats the elastic response. The maximum stress f_1' in this case is given by

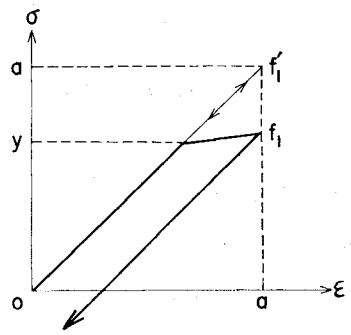

Fig. 3. Behavior of the first cycle.

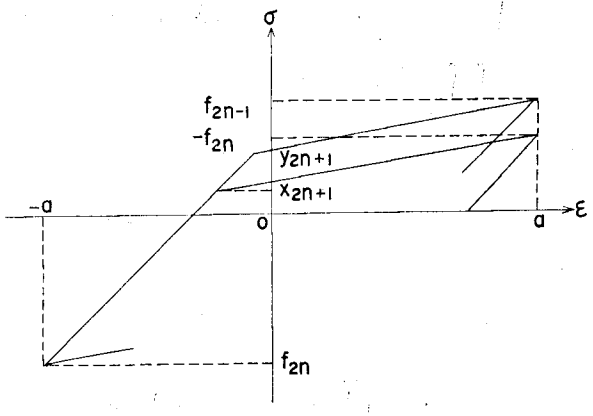

Fig. 4. Behavior of the n th cycle.

$$f_1' = \alpha \qquad \cdots\cdots(21)$$

In the general case, the hysteresis loop of the n th cycle is shown in Fig. 4. From geometrical relations indicated in this figure, we have

$$(x_{2n+1}-f_{2n})+\frac{1}{\mu}(-f_{2n}-x_{2n+1}) = 2a \qquad \cdots\cdots(22)$$

$$(y_{2n+1}-f_{2n})+\frac{1}{\mu}(f_{2n+1}-y_{2n+1}) = 2a \qquad \cdots\cdots(23)$$

Now with an assumption of a constant ζ_n during the n th cycle, eq. (13) can be rewritten as

$$\zeta_n = (x_{2n+1}-y_{2n+1})/(x_{2n+1}-(-f_{2n})) \qquad \cdots\cdots(24)$$

From eqs. (22), (23) and (24), the following relations in the ascending branch of the hystersis loop are obtained:

$$f_{2n+1} = \mu f_{2n}+(1-\mu)y_{2n+1}+2\mu a \qquad \cdots\cdots(25)$$

$$y_{2n+1} = (1-\zeta_n)x_{2n+1}-\zeta_n f_{2n} \qquad \cdots\cdots(26)$$

$$x_{2n+1} = -\frac{1+\mu}{1-\mu}f_{2n}-\frac{2\mu}{1-\mu}a \qquad \cdots\cdots(27)$$

Likewise, the n th cycle of descending branch is represented by

$$f_{2n} = \mu f_{2n-1}+(1-\mu)y_{2n}-2\mu a \qquad \cdots\cdots(28)$$

$$y_{2n} = (1-\zeta_n)x_{2n}-\zeta_n f_{2n-1} \qquad \cdots\cdots(29)$$

$$x_{2n} = -\frac{1+\mu}{1-\mu}f_{2n-1}+\frac{2\mu}{1-\mu}a \qquad \cdots\cdots(30)$$

Eliminating y_{2n}, y_{2n+1}, x_{2n}, x_{2n+1} from these six equations, we obtain

$$f_{2n+1} = -(1-2\mu\zeta_n)f_{2n}+2\mu\zeta_n a \qquad \cdots\cdots(31)$$

$$f_{2n} = -(1-2\mu\zeta_n)f_{2n-1}-2\mu\zeta_n a \qquad \cdots\cdots(32)$$

which reduce further to the following relation.

$$f_{2n+1} = (1-\mu)(\tau_y-a)\prod_{k=1}^{n}(1-2\mu\zeta_k)^2+a \qquad \cdots\cdots(33)$$

$$f_{2n} = -(1-\mu)(\sigma_y-a)(1-2\mu\zeta_n)\prod_{k=1}^{n-1}(1-2\mu\zeta_k)^2+a \qquad \cdots\cdots(34)$$

$$y_{2n+1} = (1+\mu-2\mu\zeta_n)(1-2\mu\zeta_n)(\tau_y-a)\prod_{k=1}^{n-1}(1-2\mu\zeta_k)^2 \qquad \cdots\cdots(35)$$

$$y_{2n} = -(1+\mu-2\mu\zeta_n)(\sigma_y-a)\prod_{k=1}^{n-2}(1-2\mu\zeta_k)^2-a \qquad \cdots\cdots\cdots\cdots(36)$$

4.2. The behavior of an assembly of elements

The hysteresis response of a materail subjected to a cyclic strain amplitude is represented as the sum of the contribution of each element. The elements of the material at a certain instant, when the strain is ε in the n th cycle, are classified into three groups as shown in Fig. 5. The first group (AB) remains in the elastic stage. Although displaying the elasto-plastic behavior during the whole n th cycle, the second (FGH) is still in the elastic range at this instant. The third (CDE) groups is already plastic at the level ε. These three groups are called e-type, p-e type and p-p type, respectively.

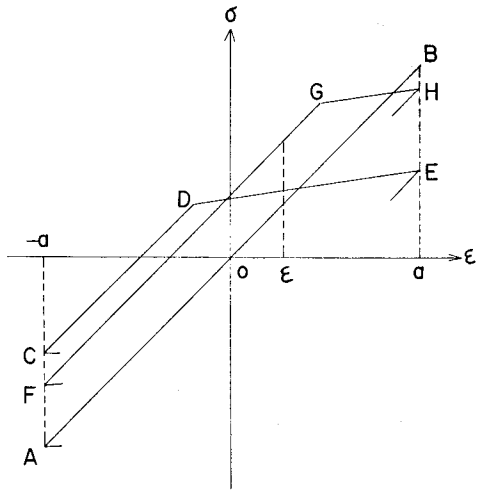

Fig. 5. Behavior of three groups; e type, p-e type and p-p type.

Apparently this classification depends on the yield level. For a given ε, the elements are divided into a p-e type and a p-p type, and the minimum yield level of the p-e type elements coincides with the maximum yield level of the p-p type elements. Let this level be denoted by r_{2n+1}.

For the p-e type elements, it holds that

$$-a<\sigma<-a+(y_{2n+1}-f_{2n}) \qquad \cdots\cdots\cdots\cdots(37)$$

Substitution from eqs. (34) and (35) leads to

$$a>\sigma_y>a-\frac{a-\varepsilon}{2(1-\mu\zeta_n)(1-2\mu\zeta_n)\prod_{k=1}^{n-1}(1-2\mu\zeta_k)^2} \qquad \cdots\cdots\cdots\cdots(38)$$

in which the right hand side conicides with r_{2n+1}; i.e.,

$$r_{2n+1} = a - \frac{a-\varepsilon}{2(1-\mu\zeta_n)(1-2\mu\zeta_n)\prod_{k=1}^{n-2}(1-2\mu\zeta_k)^2} \quad \cdots\cdots(39)$$

The ranges of σ_y outside that defined by eq. (38) specify e type and p-p type elements.

(i) e type $\sigma_y > a$; $\sigma = \varepsilon$ ……(40)

(ii) p-e type $r_{2n+1} < \sigma_y < a$; $\sigma = (\varepsilon+a)+f_{2n}$ ……(41)

(iii) p-p type $0 < \sigma_y < r_{2n+1}$; $\sigma = \mu(\varepsilon-a)+f_{2n+1}$ ……(42)

The lower brach can also be treated in a similar way, and we obtain

(iv) e type $-\sigma_y < -a$; $\sigma = \varepsilon$ ……(43)

(v) p-e type $-r_{2n} < \sigma_y < a$; $\sigma = (\varepsilon-a)+f_{2n-1}$ ……(44)

(vi) p-p type $0 < \sigma_y < -r_{2n}$; $\sigma = \mu(\varepsilon+a)+f_{2n}$ ……(45)

$$r_{2n} = -a + \frac{a+\varepsilon}{2(1-\mu\zeta_n)\prod_{k=1}^{n-1}(1-2\mu\zeta_k)^2} \quad \cdots\cdots(46)$$

From the foregoing discussions the hysteresis loop in the n th cycle is represented by

$$F_n^+(\varepsilon) = B_e + B_{pe} + B_{pp} \quad \cdots\cdots(47)$$

for the upper branch, and

$$F_n^-(\varepsilon) = C_e + C_{pe} + C_{pp} \quad \cdots\cdots(48)$$

for the lower branch, in which

$$B_e = \int_a^\infty \int_{\sigma_y}^\infty \varepsilon\varphi(\sigma_u, \sigma_y)d\sigma_u d\sigma_y \quad \cdots\cdots(49)$$

$$B_p = \int_{r_{2n+1}}^a \int_{-f_{2n}}^\infty \{(\varepsilon+a)+f_{2n}\}\varphi(\sigma_u, \sigma_y)d\sigma_u d\sigma_y \quad \cdots\cdots(50)$$

$$B_{pp} = \int_0^{r_{2n+1}} \int_{f_{2n+1}}^\infty \{\mu(\varepsilon-a)+f_{2n+1}\}\varphi(\sigma_u, \sigma_y)d\sigma_u d\sigma_y \quad \cdots\cdots(51)$$

$$C_e = B_e$$

$$C_{pe} = \int_{-r_{2n}}^a \int_{f_{2n-1}}^\infty \{(\varepsilon-a)+f_{2n-1}\}\varphi(\sigma_u, \sigma_y)d\sigma_u d\sigma_y \quad \cdots\cdots(52)$$

$$C_{pp} = \int_0^{-r_{2n}} \int_{-f_{2n}}^\infty \{\mu(\varepsilon+a)+f_{2n}\}\varphi(\sigma_u, \sigma_y)d\sigma_u d\sigma_y \quad \cdots\cdots(53)$$

Therefore the stress amplitudes L_n^+ and L_n^- at the strain amplitude $\pm a$ are then given by

$$L_n^+ = \int_a^\infty\int_{a_y}^\infty -a\varphi(\sigma_u, \sigma_y)d\sigma_u d\sigma_y + \int_0^a\int_{-f_{2n}}^\infty f_{2n}\varphi(\sigma_u, \sigma_y)d\sigma_u d\sigma_y \quad \cdots\cdots(54)$$

$$L_n^- = \int_a^\infty\int_{\sigma_y}^\infty a\varphi(\sigma_u, \sigma_y)d\sigma_u d\sigma_y + \int_0^a\int_{f_{2n-1}}^\infty f_{2n-1}\varphi(\sigma_u, \sigma_y)d\sigma_u d\sigma_y \quad \cdots\cdots(53)$$

The hysteresis area (dissipated energy per cycle) E_n is obtained as

$$E_n = \int_{-a}^{a}\{F_n^+(\varepsilon) - F_n^-(\varepsilon)\}d\varepsilon \quad \cdots\cdots(56)$$

The survival ratios R_n^+ and R_n^- of the elements under repeated loads are defined as follows:

$$R_n^+ = \int_a^\infty\int_{\sigma_y}^\infty \varphi(\sigma_u, \sigma_y)d\sigma_u d\sigma_y + \int_0^a\int_{-f_{2n}}^\infty \varphi(\sigma_u, \sigma_y)d\sigma_u d\sigma_y \quad \cdots\cdots(57)$$

$$R_n^- = \int_a^\infty\int_{\sigma_y}^\infty \varphi(\sigma_u, \sigma_y)d\sigma_u d\sigma_y + \int_0^a\int_{f_{2n-1}}^\infty \varphi(\sigma_u, \sigma_y)d\sigma_u d\sigma_y \quad \cdots\cdots(58)$$

5. Numerical results and discussion

Plastic bending fatigue tests on H-section SS 41 steel element were carried out in order to verify the applicability of the hysteresis model proposed in this study. The detail of this test is shown in reference (6).

In the numerical computations in this chapter, the following data are adopted from the test results; that is, the ultimate ductility fator $=50$, and the hardening factor $\mu=0.01$.

It must be noted that the hardening rate factor ζ which should be determined as a function of the strain amplitude a and the number of load cycles N through the microscopic mechanism. For simplicity, two different values are assigned to ζ; namely ζ_a and ζ_b, which control the initial strain hardening process and the deteriorating process to failure, respectively.

The parameters ζ_a and ζ_b are determined from the number of cycles needed to finish strain hardening and the number of cycles to the fatigue failure;

$$\zeta_a = \left\{\begin{array}{ll} 0.3+\dfrac{0.338}{a-1}; & a\geqq 1.54 \\ 1 & ; a<1.54 \end{array}\right\}; \ n\leq n^* \quad \cdots\cdots(59)$$

$$\zeta_b = \frac{a^{1.54}}{3.68\times 10^2}; \ n>n^* \quad \cdots\cdots(60)$$

Eqs. (59) and (60) are illustrated in Fig. (6).

The two dimensional desnity function $\phi(\sigma_u, \sigma_y)$ related by σ_u and σ_y is assumed to have a form shown in Fig. 7.

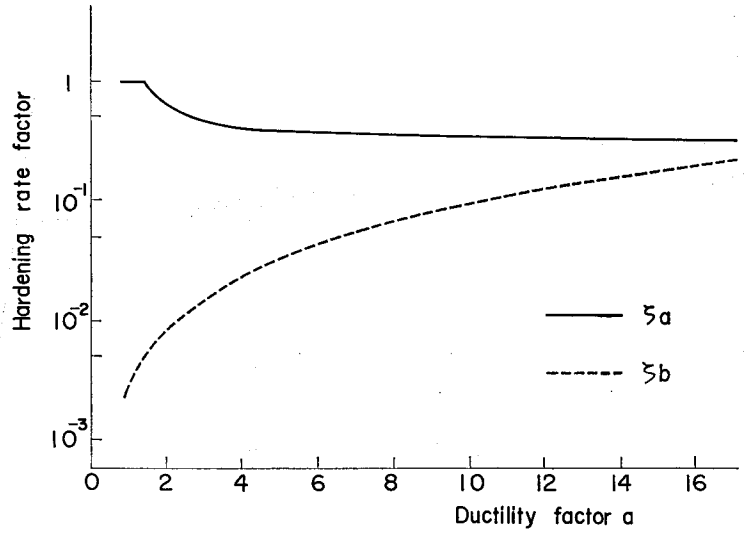

Fig. 6. Hardening rate factor.

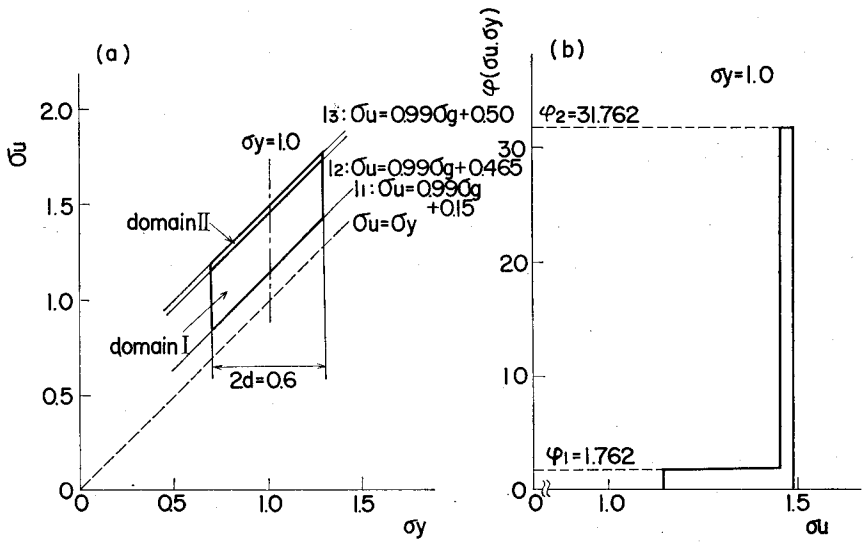

Fig. 7. Density function $\varphi(\sigma_u, \sigma_y)$.

5.1. Monotonic loading curve

Numerical computation of eq. (17) gives the monotonic loading curve $F(\varepsilon)$ shown in Fig. 8. A round corener near the yield point is due to a result of the two

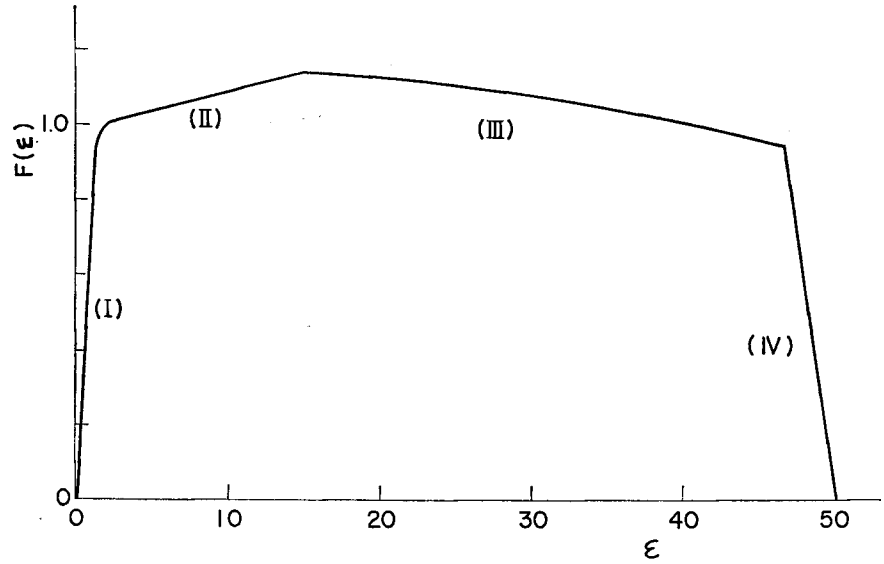

Fig. 8. Monotonic loading curve.

dimensional desnity function $\phi(\sigma_u, \sigma_y)$ which is easily controlled by using the parameter d in Fig. 7.

This curve consists of the initial elastic part I, the hardening part II at $1 \leq \varepsilon < 15.0$, the deteriorating part III at $15.0 \leq \varepsilon < 46.5$ and the final state IV at $\varepsilon \geq 46.5$.

5.2. Hysteresis loop

As it is very complicated to make a numerical analysis for an exact flexible model of the H-shaped cross section on the basis of eqs. (47) and (48), some simplification was made to compare the numerical results to the experimental results. That is, the flange section is assumed to receive only the cyclic tensile or compressive stress by neglecting the web.

This assumption may be questionable in the quantitative evaluation of the absolute stress amplitude. However, it may be sufficient to know the tendency of the fatigue failure process of the hysteresis loop.

Fig. 9 shows examples of the hysteresis loop with the input amplitudes in ductility factor $a=2.02$ and 2.37.

The theoretical result shows a more obvious yield point and a thinner overall shape of the hysteresis loop than the experimental results. These differences are because the elements of the hysteresis model herein are distributed in parallel manner. This is because surviving elements after repeated loading display their

extreme characteristics.

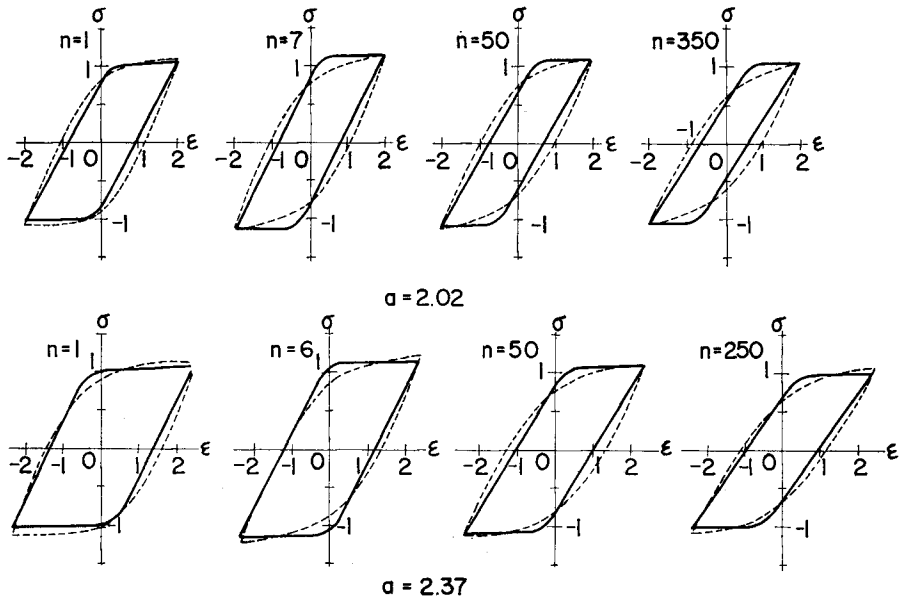

Fig. 9. Hysteresis loops.

5.3. Relation between number of cycle, reaction and dissipated energy per cycle

The variation of the hysteresis loop is investigated with the aid of the reaction amplitude and the dissipated energy per cycle in Fig. 10 showing the theoretical curves and the experimental plots. The variation of the reaction shows good agreement between the theoretical and the experimental results. However, in the theoretical results of the dissipated energy per cycle, the deterioration of the energy capactity begins about the time of the termination of the strain hardening, while in the experimental results, the deterioration proceeds from the beginning of load cycles.

The theoretical values of dissipative energy per cycle in the deteriorating range are less than the experimental values, which might be related to the way of reducing the area of hysteresis loops in the theoretical model.

The chain curve in this figure, which means the survival ratio of the material elements, shows that a part of relatively weak elements fails in its initial period $n \leq n^*$, but the other elements remain safe for a relative long period, $n > n^*$ and they fail at a very low rate until sudden rapture takes place.

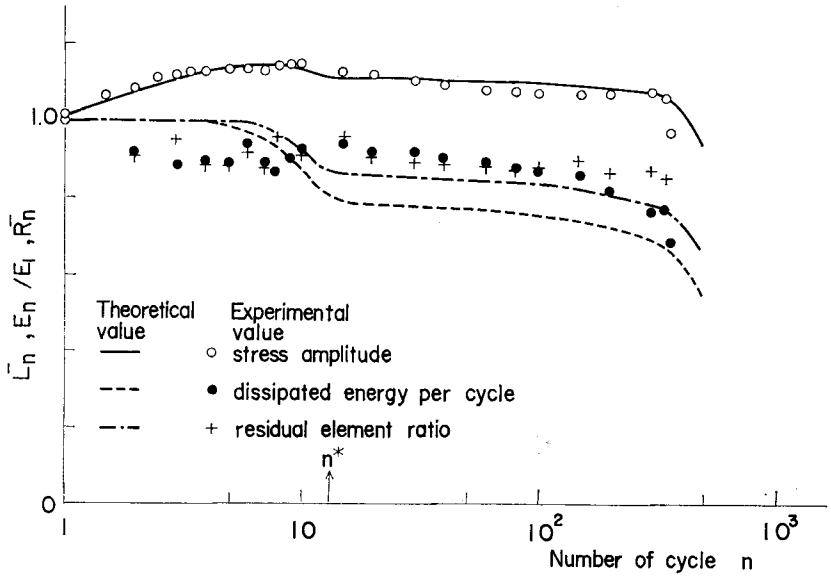

Fig. 10. Relation between number of cycle, reaction and dissiplated energy per cycle (a=2.02)

5.4. S-N curve

The solid line in Fig. 11 shows the *S-N* curve obtained from the theoretical model, and the dotted line, from the experimental results. The theoretical curve shows that the number of cycles tends to infinity as the input ductility factor a

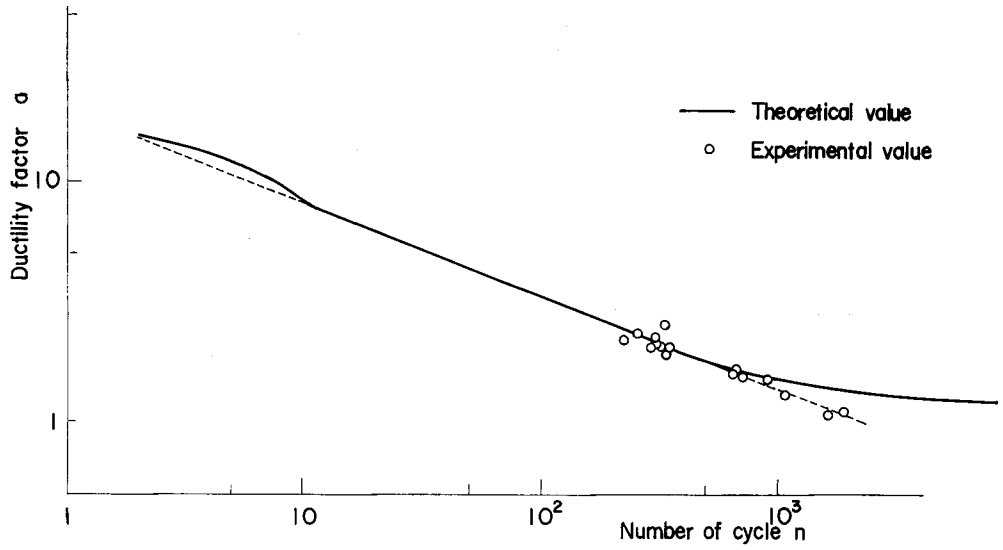

Fig. 11. S-N relation.

approaches 1. This is a consequence dependent on neglecting the fatigue due to elastic strain amplitude.

6. Conclusions

A hysteresis model was presented which can represent the plastic fatigue failure process of the engineering materials. Numerical results based on this model were compared with the experimental results of a plastic bending fatigue test on *SS* 41 *H*-section steel beams.

The following results have been obtained.

(1) The hysteresis model proposed herein can display the fatigue failure process of material which hardens in its initial stage, and deteriorates in the second stage until complete failure occurs.
Its pattern can follow the basic features of experimental results.

(2) Using this hysteresis model, any softening type materials can be dealt with. These materials will be carried out by an adequate selection of relevant parameters.

(3) This hysteresis model includes the bi-linear model ($\eta_n=0$, $d=0$) or Ramberg-Osgood model ($\zeta_n=0$, $d\neq 0$) in special case.

(4) This hystereis model is formulated as a deterministic model. However, it may be developed to a stochastic model, with the hardening rate factor redefined as a probabilistic parameter.

Acknowledgement

The authers are grateful to Professor Hisao Goto for his generous advice and encouragement given throughout the present study. It is acknowledged that the numerical computations in this study have been made on the digital computer FACOM 230–75 of the Data Processing Center, Kyoto University.

Reference

1) E. Orowan: Proc. Roy. Soc. London, A171 1939 p 79.
2) R. Tanabashi, et al: Trans. of A.I.J. No. 175 Sept. 1970 pp. 17–26.
3) J. M. Kelly and P. P. Gillis: "Constitutive Models for Cyclic Plastic Deformation of Engineering Materials." Report No. EERC 73–21 Sept. 1973 California.
4) T. Yokobori: "Strength, Fracture and Fatigue of Materials" Gihodo LTD. Japan (in Japanese) 1955.
5) T. Yokobori: Journal of the J.S.M.E. Vol. 65, No. 524 Sept. 1962 pp. 1206–1211.
6) H. Goto, et al.: "A Consideration on Failure Process of Structural Steel under Repeated Flexural Loads." Bulletin of the Disaster Prevention Research Institute No. 17, April, 1974 pp. 157–169.